Measurements and Predictions of the Aerosol Dynamics of Smoke

Amy Mensch, Haley Hamza, and Thomas Cleary
amy.mensch@nist.gov (301) 975-6714
National Institute of Standards and Technology
100 Bureau Drive, Mail Stop 8664, Gaithersburg, MD 20899

Introduction

Better understanding and ability to predict the aerosol dynamics of soot can improve life safety predictions generated by fire modeling tools. NIST's fire modeling tool, Fire Dynamics Simulator (FDS), is commonly used by the international fire protection community for design of smoke handling systems and smoke detector activation studies, as well as fire reconstructions [1]. FDS includes sub-models for aerosol transport, deposition and coagulation based on well-established correlations for spherical particles [2]–[4], while soot from flaming fires is generically characterized as a fractal structure of agglomerated 0.02 µm – 0.04 µm diameter primary particles. The appropriate characteristic size of a soot agglomerate depends on what is being characterized, i.e., inertial drag, coagulation, or thermophoresis. For coagulation, the number of bins specified to represent the actual distribution of particle sizes also requires consideration of the needs for prediction accuracy and computational efficiency. The soot dynamics sub-models in FDS and the soot parameters specified for the simulation all impact soot-related predictions, which include surface deposition, smoke alarm activation, visibility, and tenability.

Aerosol transport mechanisms that are often present and important in fire environments include gravitational, turbulent diffusion, and thermophoresis. In fire experiments where soot deposition was measured [5], [6], contributions from multiple mechanisms make it difficult to use the results to validate any one mechanism. However, for a standard heptane fire (EN 54 part 9 [7]), Rexfort [8] was able to show an improvement in the FDS predictions of soot concentration with particle coagulation modeled, particularly after the fire was extinguished.

Another approach to isolate deposition mechanisms is to introduce post-flame soot into a non-reacting environment with well characterized flow and thermal conditions. The contributions from thermophoretic deposition were isolated using a laminar flow channel with opposing hot and cold surfaces in Mensch and Cleary [9]. Within the uncertainties, the measurements matched the FDS predictions when using the soot's primary particle diameter in the thermophoretic equations. Mensch and Cleary [10] also constructed a ~1.5 m^3 cubic isothermal enclosure with a fan in the center directing flow upward to evaluate gravitational deposition, turbulent deposition and coagulation. Initial experiments, conducted for spherical particles of known size distributions, monitored the decay in aerosol concentration over time. The results showed good agreement for low fan flow rates and high particle concentrations, cases when coagulation dominated over deposition.

The current study builds upon the previous spherical particle study [10] to quantify the concentration decay of two different aerosols, which simulate smoke from smoldering fires and soot from flaming fires, under quiescent flow. The experimental scenarios are simulated in FDS to demonstrate a possible approach for handling the coagulation of smoke in practical fire scenarios. The FDS predictions are compared to the experimental results to evaluate the limitations of the current FDS models and the proposed treatment for soot agglomerates.

Experimental Methods

The ~1.5 m^3 cubic enclosure used in the previous well-stirred experimental study [10] is again used for the current isothermal aerosol experiments to study the coagulation of two different types of aerosol particles in quiescent flow conditions, to minimize turbulent deposition losses. The first aerosol simulate smoke from smoldering fires with spherical mineral oil droplets generated by a Gemini Smoke Detector Analyzer[1], originally developed to test smoke detectors [11]. The second aerosol was fractal-like soot particles, generated by burning propene in a laminar diffusion flame burner with co-flow air [12]. The propene flowrate was 1.3 E-6 m^3/s (0.077 L/min), and the co-flow air flowrate was 9.02 E-4 m^3/s (54.1 L/min). The burner was enclosed by a brass chimney that contained a tripper plate to induce mixing followed by the injection of 32.5 L/min of additional dilution air. All fuel and air flowrates for the burner were set by mass flow controllers with a manufacturer reported uncertainty of ± 1 %. Before introduction into the enclosure, the soot also passed through a charge neutralizer.

A micro-orifice low pressure cascade impactor [13] was used to measure the initial aerodynamic size distributions of each aerosol. The aerodynamic diameter is defined as the equivalent diameter of a sphere with a density of 1000 kg/m^3 (1 g/cm^3) that has the same inertial characteristics of the real particle. The aerodynamic size distributions of the mineral oil and soot aerosols are shown in Fig. 1 with the open symbols. For mineral oil, the mass median aerodynamic diameter (MMAD) is 0.35 µm with a geometric standard deviation (GSD) of 1.37. For soot, the MMAD is 0.29 µm with a GSD of 2.42. The aerodynamic sizes can be converted to physical sizes, which are relevant for coagulation, by applying a density correction and applying slip corrections for size smaller than 10 µm. The mineral oil (simulated smolder smoke) droplets have a measured bulk density of 830 kg/m^3 (0.83 g/cm^3). Although the bulk density of soot is 1800 kg/m^3 (1.8 g/cm^3), an effective density of 200 kg/m^3 (0.2 g/cm^3) is used to compute the physical size to account for the sparseness of primary particles in the structure of soot. The resulting physical size distributions, useful for coagulation computations, are shown in Fig. 1 with filled symbols. The measured values for physical size, represented as mass median diameter (MMD) and GSD, of both mineral oil and soot are listed in Table 1.

Both aerosols were introduced into the enclosure through an inlet port located 0.3 m from the base of the enclosure, and a fan in the center of the enclosure circulated flow around the box to evenly distribute the aerosol during the filling stage, shown in Fig. 2. The fan was turned off for the two-hour (7200 s) experiment to track the decay in aerosol concentration, primarily due to coagulation. A sample tube, also shown in Fig. 2, pointed vertically up inside the enclosure extracted the aerosols at a location that was 0.3 m from the side wall, and 0.6 m from the base. The particle number concentration, N, was continuously monitored by a condensation particle counter (CPC), which pulled 5 E-6 m^3/s (0.3 L/min) through the sample tube. Before the beginning and after the end of the two-hour experiment, the sample tube was also connected to a tapered element oscillating microbalance (TEOM) to measure the initial and final mass concentration. The TEOM pulled an additional 5 E-5 m^3/s (3 L/min) from the enclosure. Both the CPC and the TEOM record data at a rate of 1 Hz, and the initial measurements of number and mass concentration are in Table 1. Filtered ambient air was allowed to enter the enclosure through the make-up flow inlet.

[1] Certain commercial equipment, instruments, or materials are identified in this paper in order to specify the procedures adequately. Such identification is not intended to imply recommendation or endorsement by the National Institute of Standards and Technology, nor is it intended to imply that the materials or equipment identified are necessarily the best available for the purpose.

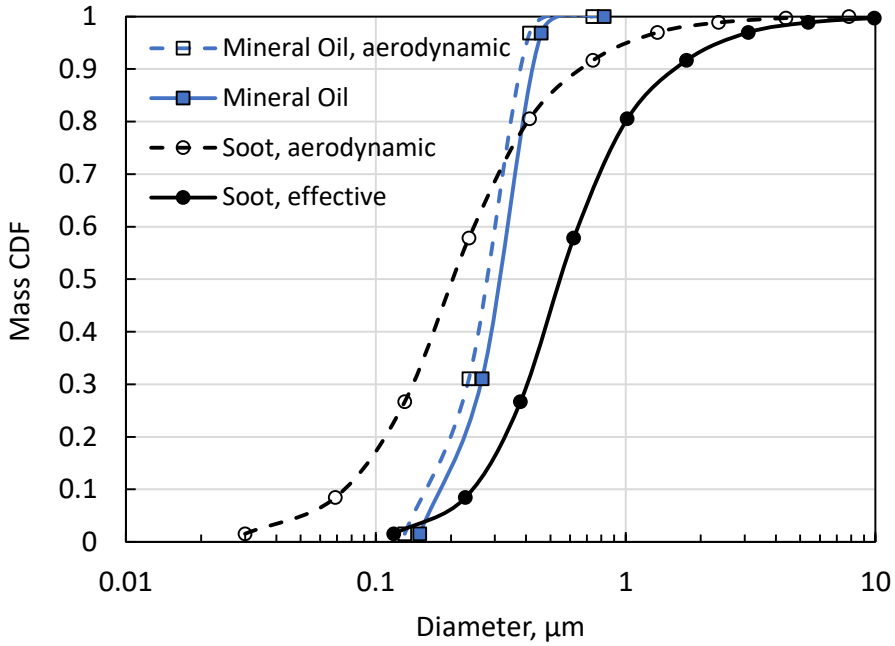

Fig. 1. Mass cumulative distribution function of particle diameters for both mineral oil and soot aerosols before aging in the enclosure, as measured by a micro-orifice low pressure cascade impactor.

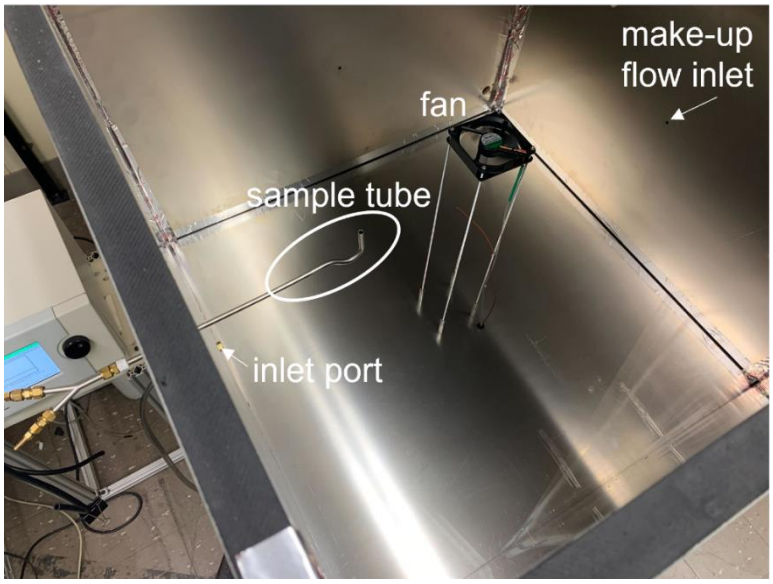

Fig. 2. Photo looking down into the isothermal enclosure, with inlet port, sample tube, fan, and makeup flow inlet labelled.

Computational Modeling

FDS simulations of aerosol coagulation were conducted to track the predicted changes in aerosol particle concentration in quiescent flow in the isothermal enclosure. All simulations used a uniform rectangular grid of 1.5 E6 cells, each with dimensions 0.01 m. Aerosol size distributions were represented by a finite number of bins to compute the effects of particle coagulation. The number of bins used can affect the accuracy and efficiency of the solutions. Therefore, an initial

bin study was performed for a generic aerosol to inform the number of bins to use in the simulations of the mineral oil and soot experiments.

Bin Study

An initial series of coagulation simulations were conducted using FDS version 6.7.1 to examine the effect of the number of bins used to represent generic aerosols with a bulk density of 1000 kg/m^3. Three different sizes, with log-normal distributions about geometric mean diameters (GMD) of 0.25 µm, 1 µm, and 4 µm, all with a GSD of 1.6, were all represented with 3 bins, 5 bins, 9 bins, and 15 bins. The initial set of simulations were set up to age the aerosols in the isothermal enclosure without deposition and with coagulation only due to Brownian diffusion. The final number concentration normalized by the initial number concentration, N/No, and final GMD, after 1000 s and after 10,000 s were compared to the analytical solution for Brownian coagulation from Park et al. [14].

The final N/No results for all sizes and all numbers of bins are compared to the analytical solution in Fig. 3. The cases with 15 bins and 9 bins were within 15 % of the analytical solution in most cases, and the cases with 5 bins also resulted in relatively good predictions, with the largest differences occurring for the smallest GMD of 0.25 µm. The 3 bins predictions had significant errors for some conditions because of the lack of resolution in the size distribution with only 3 bins. The increases in computational times compared to 3 bins were 16 %, 60 %, and 240 % for 5 bins, 9 bins and 15 bins, respectively. A second set of simulations included circulating flow from the fan and particle losses due to gravitational and turbulent deposition in addition to coagulation. Details about modeling the fan flow can be found in Mensch and Cleary [10]. With flow and deposition, the 5 bins and 9 bins predictions for final N/No and final GMD were within 10 % of the 15 bins predictions (flow cases did not have an analytical solution).

Simulations of Mineral Oil and Soot Experiments

The quiescent aging experiments were modeled in FDS for the mineral oil and soot aerosols represented in Fig. 1. The FDS simulations, conducted with version 6.7.9, modeled the aerosol dynamics of particle coagulation, wall deposition losses due to gravitational and turbulent deposition, and dilution losses due to sample and make-up flows. The sample tube was modeled with a rectangular obstruction, extending from the wall to the approximate location of the sample tube opening in the experiment. The sample flow (5.0 E-6 m^3/s) was removed at the obstruction's interior face, and clean air entered through an open boundary on the opposite wall of the enclosure at the make-up flow inlet location. The parameters used to model the aerosols in the FDS cases are given in Table 1. Two cases were run for each aerosol type, using 5 bins and 8 bins to represent the particle size distributions and compute particle coagulation. The minimum and maximum sizes for the bins were specified to cover three GSD's from the MMD, using the measured values. The initial mass concentration from the experiments was distributed into the five or eight FDS bins assuming a log-normal distribution. The results from the initial time step showed that the MMD, GSD, and total mass concentration were accurately represented by the FDS bins (< 2 % error). Number concentrations were computed from the mass concentration per bin, the bulk density and the bin sizes, and summing the number concentrations per bin. The computed No were significantly different from the measurements due to the sensitivity to accurate representation of the smallest sizes of the distribution. For mineral oil, the difference is due to measurement uncertainties in the masses on the smallest stages of the cascade impactor and imperfect representation of the smallest sizes when converting the impactor measurements to the pre-defined

FDS bins assuming a log-normal distribution. For soot, the use of a much lower effective density also significantly increases the computed number concentration.

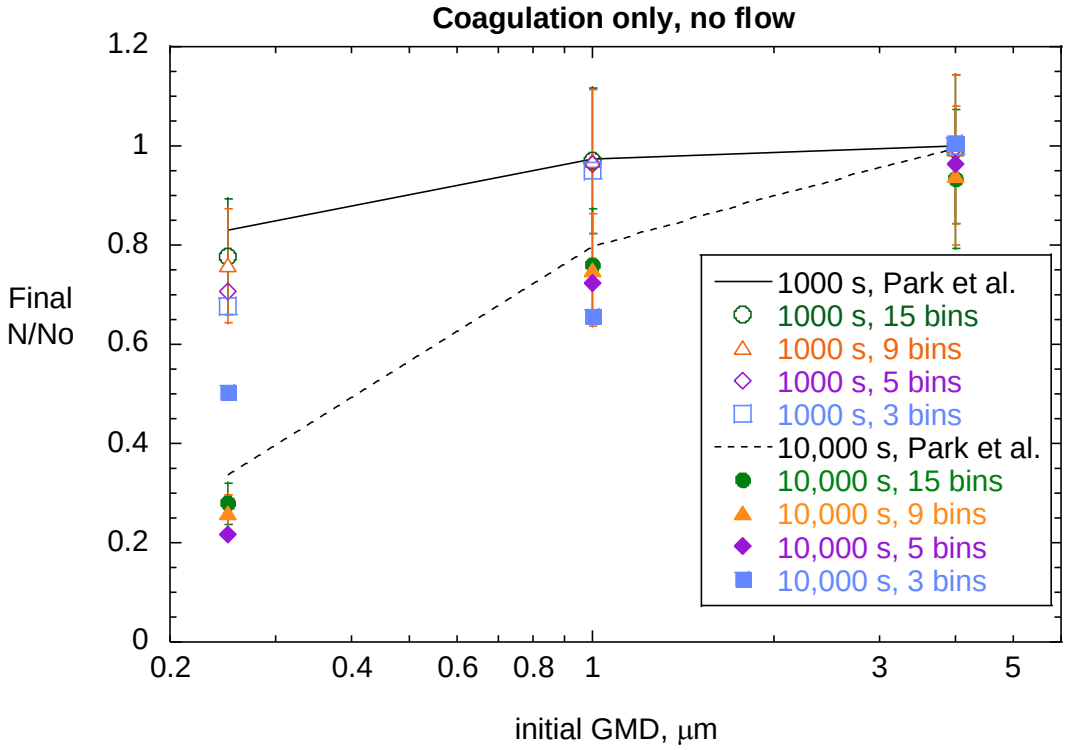

Fig. 3. Bin study results of final N/No predicted by the coagulation only FDS simulations compared to the analytical solution from Park et al. [14], with 15 % error bars shown for the cases with 15 bins and 9 bins.

Table 1. Aerosol Parameters Used for FDS Cases

Aerosol	Mineral Oil	Soot
Number of bins	5 | 8	5 | 8
Minimum bin size (μm)	0.155	0.072
Maximum bin size (μm)	1	8
Specified bulk density (kg/m^3)	830	200
Initial MMD, measured (μm)	0.392 (± 10 %)	0.760 (± 10 %)
Initial GSD, measured	1.36 (± 10 %)	2.19 (± 10 %)
Initial mass concentration, measured (kg/m^3)	5.8 E-6 (± 2 %)	6.312 E-6 (± 1 %)
Initial number concentration, No, measured (/m^3)	6.12 E11 (± 6 %)	6.03 E11 (± 11 %)
Initial number concentration, No, simulated (/m^3)	3.43 E11 | 3.36 E11	2.00 E12 | 1.82 E12

Standard measurement uncertainties, for a 95 % confidence interval, are reported in parentheses.

Results and Discussion

Mineral Oil Results

The experimental results and FDS predictions of N/No for mineral oil are shown in Fig. 4(a). The measured N/No decayed by 70 % over the 7200 s experiment to a value of 0.30. The final experimental N/No compares well with the analytical solution for Brownian coagulation from Park et al. [14], 0.32, which is represented by an x in Fig. 4(a). Because most of the decay in number concentration was due to particle coagulation, with minimal impact of deposition and make-up flow dilution, the measured mass concentration only reduced by 6 % to 5.43 E-6 kg/m^3 (± 1 %).

The FDS predictions of N/No decayed less than the experiment, with little difference in the predictions between the 5 bins and 8 bins cases. The differences in N/No between the experiment and FDS can be attributed to the lower initial No for the FDS simulations. Because coagulation is proportional to the square of the number concentration, FDS predicts less coagulation than is observed in the experiment. Using the starting No values computed for the FDS cases, the analytical solution and FDS predictions matched at 7200 s, as shown in Fig 4(a). FDS predicted a shift in the mineral oil size distribution due to coagulation, increasing the MMD to about 0.5 µm (30 % increase from the initial MMD). The GSD was predicted to stay about the same. The FDS predictions of the final mass concentration were within 2 % of the final measurement, confirming that FDS accurately predicted the deposition and dilution effects.

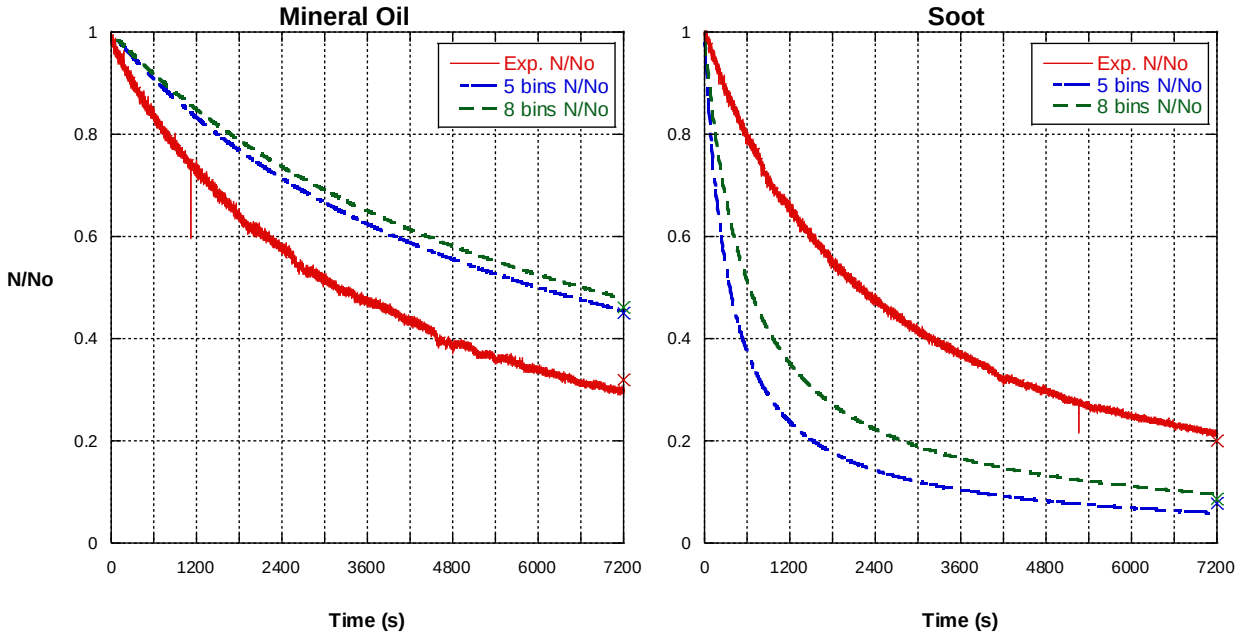

Fig. 4. Decay in relative particle number concentration, N/No, over the experiment compared to FDS predictions using 5 bins and 8 bins for the size distributions of (a) mineral oil and (b) soot. The coagulation-only analytical solutions [14] are shown with the x symbols at 7200 s.

Soot Results

The N/No results from the experiments and FDS simulations are shown in Fig. 4(b). The soot N/No decayed to a final measured value of 0.22 over the duration of the experiment. This measurement compared well with the coagulation-only analytical prediction of 0.20, using the effective density of 200 kg/m^3. If, instead, the solid bulk density of 1800 kg/m^3 was used, the Park et al. analytical solution would be 0.07 for the final N/No. Therefore, the agreement between the

experiment and the analytical solution using 200 kg/m^3 confirmed the selection of that value for an effective density of soot. Similar to mineral oil, the measured soot mass concentration only decayed by 6 % to 5.92 E-6 kg/m^3 (± 1 %). Both aerosols had similar measured initial aerodynamic diameters, so it is expected that the mineral oil and soot have similar rates of deposition.

For soot, both FDS cases predicted a greater decay in N/No than was measured, but in this case FDS began with much greater No values than the experiment. When the No values FDS started with are used, the coagulation-only analytical predictions were close to the final FDS predictions. Like mineral oil, FDS predicted a change in the soot size distribution, with a final MMD of 1.06 µm predicted from the case with 8 size bins (40 % increase from the initial MMD). The GSD was predicted to decrease about 20 % to a narrower distribution with a final GSD 1.7 for 8 size bins. The 5 bins case predicted slightly larger values for final MMD (1.29 µm) and GSD (1.8). As with mineral oil, the final soot mass concentrations predicted by FDS are only 2 % different from the soot mass concentration measured at the end of the experiment.

Conclusions

The particle aging experiments in this study tracked the coagulation of two different aerosols that are representative of smokes from smoldering fires (mineral oil) and from flaming fires (soot). The FDS simulations of the quiescent experiments demonstrated a practical method to model coagulation of smoke from fires, given that some information is known or can be inferred about the smoke morphology and size distribution. For both aerosol types, the FDS simulations predicted a minor decay in mass concentration, due to deposition and make-up flow dilution, that was consistent with the experimental measurements.

The limitations of the FDS simulations were apparent when focusing on number concentration, which needs to be computed to model coagulation dynamics. The FDS results were similar whether using 5 bins or 8 bins to represent the size distributions. The differences from the experiments for number concentration decay were not due to errors in the coagulation models. It was confirmed that FDS was accurately predicting coagulation because the results agreed with the Park et al. [14] analytical solutions for coagulation when the same No was used.

The differences from the experiments were attributed to a mismatch between the computed values of No at the start of the simulations and the measured No. The difficulty is in accurately representing the tails of the distribution when converting the distribution measurements to the bins in the simulation. Any imperfect representation of the smallest sizes in the aerosol distributions could have a significant impact on the number concentration, but very little effect on the mass concentration because the smallest particles did not contribute much to the total mass. For soot, the computed number concentration was also higher due to the use of a lower effective density of 200 kg/m^3. The lower effective density was used to approximate the apparent physical size of the non-spherical soot particles for particle coagulation. The use of this value was confirmed by the good agreement between the measured N/No and the Park et al. [14] analytical solution for coagulation using the lower effective density. Although the apparent physical sizes that were computed using this density were appropriate for coagulation, this characterization would not have been appropriate to model all soot phenomena. For example, thermophoretic deposition, which was not included in these simulations, correlates with the much smaller primary particle size, and may require the specification of an additional thermophoretic diameter in FDS.

[1] K. McGrattan, S. Hostikka, R. McDermott, J. Floyd, and M. Vanella, “Fire Dynamics Simulator User’s Guide 6th Edition,” National Institute of Standards and Technology, Gaithersburg, MD, NIST SP 1019, Jun. 2022. doi: 10.6028/NIST.SP.1019.
[2] J. Floyd, K. Overholt, and O. Ezekoye, “Soot Deposition and Gravitational Settling Modeling and the Impact of Particle Size and Agglomeration,” *Fire Safety Science*, vol. 11, pp. 376–388, 2014, doi: 10.3801/IAFSS.FSS.11-376.
[3] J. Floyd and R. McDermott, “Modeling soot deposition using large eddy simulation with a mixture fraction based framework,” in *Interflam: Proceedings of the 12th International Conference*, University of Nottingham, UK, 2010, pp. 755–764.
[4] J. Floyd, “A numerical investigation on the impact of modeling aerosol behaviors on the prediction of soot density in a compartment fire,” in *Interflam: Proceedings of the 14th International Conference*, Jul. 2016, vol. 2, pp. 835–846.
[5] S. Riahi and C. Beyler, “Measurement and Prediction of Smoke Deposition from a Fire Against a Wall,” *Fire Safety Science*, vol. 10, pp. 641–654, 2011, doi: 10.3801/IAFSS.FSS.10-641.
[6] W. D. Ciro, E. G. Eddings, and A. F. Sarofim, “Experimental and Numerical Investigation of Transient Soot Buildup on a Cylindrical Container Immersed in a Jet Fuel Pool Fire,” *Comb. Sci. and Tech.*, vol. 178, no. 12, pp. 2199–2218, Jun. 2006, doi: 10.1080/00102200600626108.
[7] *EN 54 part 9 Components of automatic fire detection systems. Methods of test of sensitivity to fire*. 2013.
[8] C. Rexfort, “Combination of a fire model and a fire sensor model,” presented at the 13th International Conference on Automatic Fire Detection, Duisburg, Germany, Sep. 2004. [Online]. Available: http://nts.uni-due.de/eusas/publications/aube_04.html
[9] A. E. Mensch and T. G. Cleary, “Measurements and predictions of thermophoretic soot deposition,” *International Journal of Heat and Mass Transfer*, vol. 143, p. 118444, Nov. 2019, doi: 10.1016/j.ijheatmasstransfer.2019.118444.
[10] A. Mensch and T. Cleary, “Validation of Aerosol Dynamics in a Well-Stirred Isothermal Enclosure,” in *Proceedings of 17th International Conference on Automatic Fire Detection (AUBE ’21) & Suppression, Detection and Signaling Research and Applications Conference (SUPDET 2021)*, Duisburg, Germany, Sep. 2021, p. 8.
[11] T. G. K. Lee, “An instrument to evaluate installed smoke detectors,” NBSIR 78–1430, Feb. 1978.
[12] T. G. Cleary, G. W. Mulholland, L. K. Ives, R. A. Fletcher, and J. W. Gentry, “Ultrafine Combustion Aerosol Generator,” *Aerosol Science and Technology*, vol. 16, no. 3, pp. 166–170, Jan. 1992, doi: 10.1080/02786829208959546.
[13] V. A. Marple, K. L. Rubow, and S. M. Behm, “A Microorifice Uniform Deposit Impactor (MOUDI): Description, Calibration, and Use,” *Aerosol Science and Technology*, vol. 14, no. 4, pp. 434–446, Jan. 1991, doi: 10.1080/02786829108959504.
[14] S. H. Park, K. W. Lee, E. Otto, and H. Fissan, “The Log-Normal Size Distribution Theory of Brownian Aerosol Coagulation for the Entire Particle Size Range: Part I—Analytical Solution Using the Harmonic Mean Coagulation Kernel,” *Journal of Aerosol Science*, vol. 30, no. 1, p. 14, 1999.